Regular Article - Theoretical Physics

Polarized semi-inclusive electroweak structure functions at next-to-leading-order

Daniel de Florian, Yamila Rotstein Habarnau[a]

Departamento de Física, FCEyN, Universidad de Buenos Aires, (1428) Pabellón 1 Ciudad Universitaria, Capital Federal, Argentina

Abstract We present a next-to-leading order (NLO) computation of the full set of polarized and unpolarized electroweak semi-inclusive DIS (SIDIS) structure functions, whose knowledge is crucial for a precise extraction of polarized parton distributions. We focus on the phenomenology of the polarized structure functions for the kinematical conditions that could be reached in an Electron-Ion-Collider. We show that the NLO corrections are sizeable, particularly in the small-x range. We test the sensitivity of these structure functions on certain quark distributions and compare it to the situation of inclusive DIS and electromagnetic SIDIS.

1 Introduction

Understanding how the nucleon spin is composed of the angular momenta and spins of its constituents (quarks and gluons) has been a defining question in hadron structure for a long time. Since it was found that little of the proton spin is carried by the quarks and anti-quarks spins, several experiments have measured with increasing precision observables which are sensitive to quark and gluon polarizations in the nucleon. Such experimental progress was matched by advancements in theoretical precision and phenomenological analyses of the data [1, 2].

The spin structure of a nucleon can be described by the (anti)quark and gluon polarized parton distribution functions (pPDFs), defined by

$$\Delta f_j(x, Q^2) \equiv f_j^+(x, Q^2) - f_j^-(x, Q^2), \tag{1}$$

where $f_j^+(x, Q^2)$ ($f_j^-(x, Q^2)$) denotes the distribution of a parton j with positive (negative) helicity in a nucleon with positive helicity, as a function of momentum fraction x and scale Q. Its first momentum, that is to say, the integral $\Delta f_j^1(Q^2) \equiv \int_0^1 \Delta f_j(x, Q^2) \, dx$, directly measures the spin contribution of the parton j to the proton spin.

The most complete global fit includes all available data taken in spin-dependent deep inelastic scattering (DIS), semi-inclusive DIS (SIDIS) with identified pions and kaons, and proton–proton collisions. They allow us to extract sets of pPDFs consistently at next-to-leading order (NLO) in the strong coupling constant along with estimates of their uncertainties [3, 4].

Unlike unpolarized PDF fits, where a clear separation of different quark flavours is possible by the use of inclusive charged-current DIS data, differences in polarized quark and anti-quark distributions are determined exclusively from SIDIS data and hence require knowledge of the hadronization mechanism, encoded in non-perturbative fragmentation functions (FFs). Pion FFs are rather well known, but uncertainties for kaon FFs are much larger. Significant progress on the quality of fits of FFs is expected once data from B factories and the LHC become available.

Despite the impressive experimental and theoretical progress made in the last years, many fundamental questions related to the proton spin structure still remain unanswered. One of the main problems is that present fixed-target experiments suffer from their very limited kinematic coverage in x and Q^2. The kinematic range could be extended in an Electron-Ion Collider (EIC), whose set-up is being currently considered [5], and thus SIDIS measurements would allow us to extract Δu, $\Delta \bar{u}$, Δd, $\Delta \bar{d}$, Δs, and $\Delta \bar{s}$ with much higher precision. Furthermore, this new collider would present the opportunity to perform DIS and SIDIS measurements via charged and neutral electroweak currents, which permits to access polarized electroweak structure functions [6–8] that depend on various combinations of polarized quark PDFs and provide an effective way of disentangling different quark flavours.

Experimentally, one has access to the asymmetries, which depend on both the polarized and the unpolar-

[a] e-mail: yrotstein@df.uba.ar

ized structure functions (g_i and F_i, respectively). The unpolarized SIDIS structure functions are well known at next-to-leading order (NLO) in perturbative Quantum-Chromodynamics (QCD) [9, 10], as well as the electromagnetic polarized ones [10]. However, polarized SIDIS structure functions for charged current and Z boson exchange are only known to leading-order accuracy (LO) [11]. In general, a LO calculation only captures the main features but does not provide a quantitative description of the process. It is then necessary to know the NLO QCD corrections to both the unpolarized and the polarized structure functions in order to extract reliable information on the parton distribution functions.

In this work we present a NLO computation of both polarized and unpolarized SIDIS structure functions. We focus on the electroweak ones, which are particularly useful to achieve a full flavour separation. The paper is organized as follows. In Sect. 2 we establish the definition of electroweak (un)polarized structure functions and present their LO expressions. In Sect. 3 we explain the main features of the computation of the structure functions at NLO, focusing on the new results for the polarized case. In Sect. 4 we present some phenomenological results and analyze the relevance of the NLO description of polarized SIDIS. Finally, we present our conclusions in Sect. 5.

2 SIDIS electroweak structure functions

In this section we establish the definition of the electroweak structure functions at lowest order in perturbation theory. We focus, in this and the following sections, on the semi-inclusive case, leaving some comments on the totally inclusive DIS to Appendix B. For more details on DIS notation, we refer to [12].

In lowest-order perturbation theory of electroweak interactions, the cross section for the scattering of polarized leptons on polarized nucleons and the consequent observation of a hadron H in the final state, can be expressed in terms of the product of a leptonic and a hadronic tensor as

$$\frac{d\sigma^H}{dx\,dy\,dz} = \frac{2\pi y\alpha^2}{Q^4} \sum_j \eta_j L_j^{\mu\nu} W_{\mu\nu}^{H,j}, \qquad (2)$$

where x and y denote the usual DIS variables, $-q^2 = Q^2 = Sxy$, $x = Q^2/(2P \cdot q)$ (q being the electroweak current four-momentum, and S the center-of-mass energy squared of the lepton-nucleon system) and $z = P_H \cdot P/P \cdot q$ the scaling variable representing the momentum fraction taken by the hadron H.[1] For neutral-current (NC) processes, the

sum runs over $j = \gamma$, Z and γZ, representing photon and Z exchange and the interference between them respectively, while for charged-current (CC) processes the interaction occurs only via the exchange of a W boson ($j = W$). The tensor $L^{\mu\nu}$ is associated with the coupling of the exchanged boson to the leptons, and the hadronic tensor $W_{\mu\nu}^H$ describes the interaction of the appropriate electroweak currents with the target nucleon and the subsequent hadronization of partons into H. The factors η_j denote the ratios of the corresponding propagators and couplings to the photon propagator and coupling as

$$\eta_\gamma = 1; \qquad \eta_{\gamma Z} = \left(\frac{G_F M_Z^2}{2\sqrt{2}\pi\alpha}\right)\left(\frac{Q^2}{Q^2 + M_Z^2}\right);$$

$$\eta_Z = \eta_{\gamma Z}^2; \qquad \eta_W = \frac{1}{2}\left(\frac{G_F M_W}{4\pi\alpha}\frac{Q^2}{Q^2 + M_W^2}\right)^2. \qquad (3)$$

The unpolarized and polarized SIDIS structure functions (F_i^H and g_i^H respectively) are defined in terms of the hadronic tensor [12]

$$W_{\mu\nu}^{H,j} = \left(-g_{\mu\nu} + \frac{q_\mu q_\nu}{q^2}\right) F_1^{H,j}(x, z, Q^2)$$

$$+ \frac{\hat{P}_\mu \hat{P}_\nu}{P \cdot q} F_2^{H,j}(x, z, Q^2)$$

$$- i\epsilon_{\mu\nu\alpha\beta} \frac{q^\alpha P^\beta}{2P \cdot q} F_3^{H,j}(x, z, Q^2)$$

$$+ i\epsilon_{\mu\nu\alpha\beta} \frac{q^\alpha}{P \cdot q}\left[S^\beta g_1^{H,j}(x, z, Q^2)\right.$$

$$+ \left(S^\beta - \frac{S \cdot q}{P \cdot q} P^\beta\right) g_2^{H,j}(x, z, Q^2)\right]$$

$$+ \frac{1}{P \cdot q}\left[\frac{1}{2}(\hat{P}_\mu \hat{S}_\nu + \hat{S}_\mu \hat{P}_\nu) - \frac{S \cdot q}{P \cdot q}\hat{P}_\mu \hat{P}_\nu\right]$$

$$\times g_3^{H,j}(x, z, Q^2)$$

$$+ \frac{S \cdot q}{P \cdot q}\left[\frac{\hat{P}_\mu \hat{P}_\nu}{P \cdot q} g_4^{H,j}(x, z, Q^2) + \left(-g_{\mu\nu} + \frac{q_\mu q_\nu}{q^2}\right)\right.$$

$$\times g_5^{H,j}(x, z, Q^2)\right], \qquad (4)$$

where P and S denote the nucleon momentum and spin four-vectors respectively and $\hat{P}$, $\hat{S}$ are

$$\hat{P}_\mu = P_\mu - \frac{P \cdot q}{q^2}q_\mu, \qquad \hat{S}_\mu = S_\mu - \frac{S \cdot q}{q^2}q_\mu. \qquad (5)$$

The spin-averaged SIDIS cross section for $e^\pm N$ scattering and the subsequent production of a hadron H in the current fragmentation region, for $Q^2 \gg M^2$ (where M is the mass of the nucleon), is given in terms of the unpolarized

---

[1] We point out that we concentrate here in the current fragmentation region, and thus cuts over the z variable must be imposed (typically, $z > 0.1$). For a description of this process in the target fragmentation region, see Refs. [13–15].

structure functions by

$$\frac{d\sigma^{H,i}}{dx\,dy\,dz} = \frac{2\pi\alpha^2}{xy Q^2}\eta^i\Big[[1+(1-y)^2]2x F_1^{H,i}$$
$$\mp[1-(1-y)^2]x F_3^{H,i} + (1-y)2F_L^{H,i}\Big], \quad (6)$$

where i corresponds to NC or CC. The longitudinal structure function is defined as $F_L^H = F_2^H - 2x F_1^H$ and vanishes at lowest order according to the Callan–Gross relation [16]. $\eta^{NC} = 1$, while $\eta^{CC} = (1\pm\lambda)^2\eta_W$ (η_W defined in Eq. (3)), where $\lambda = \pm 1$ represents the electron/positron helicity. (For incoming neutrinos, it is $\eta^{CC} = 4\eta_W$ instead.) Here and in what follows, the sign $\pm$ refers to the lepton charge.

The NC structure functions can be obtained as the sum of the photon, Z, and interference contributions:

$$F_{1,L}^{H,NC} = F_{1,L}^{H,\gamma} - (g_V^e \pm \lambda g_A^e)\eta_{\gamma Z}F_{1,L}^{H,\gamma Z}$$
$$+ (g_V^{e\,2} + g_A^{e\,2} \pm 2\lambda g_V^e g_A^e)\eta_Z F_{1,L}^{H,Z} \quad (7)$$

and

$$x F_3^{H,NC} = -(g_A^e \pm \lambda g_V^e)\eta_{\gamma Z}x F_3^{H,\gamma Z}$$
$$+ [2g_V^e g_A^e \pm \lambda(g_V^{e\,2} + g_A^{e\,2})]\eta_Z x F_3^{H,Z}, \quad (8)$$

with $g_V^e = -\frac{1}{2} + 2\sin^2\theta_W$, $g_A^e = -\frac{1}{2}$.

For the case of a polarized target, the difference $\Delta\sigma$ of cross sections for the two nucleon helicity states is

$$\frac{d\Delta\sigma^{H,i}}{dx\,dy\,dz} = \frac{8\pi\alpha^2}{xy Q^2}\eta^i\Big[[1+(1-y)^2]x g_5^{H,i}$$
$$\pm[1-(1-y)^2]x g_1^{H,i} + (1-y)g_L^{H,i}\Big], \quad (9)$$

where again i corresponds to NC or CC and where $g_L^H = g_4^H - 2x g_5^H$. Like F_L, the latter vanishes at leading order. The NC spin dependent structure functions are

$$g_1^{H,NC} = \pm\lambda g_1^{H,\gamma} - (g_A^e \pm \lambda g_V^e)\eta_{\gamma Z}g_1^{H,\gamma Z}$$
$$+ (2g_V^e g_A^e \pm \lambda(g_V^{e\,2} + g_A^{e\,2}))\eta_Z g_1^{H,Z},$$
$$g_{5,L}^{H,NC} = -(g_V^e \pm \lambda g_A^e)\eta_{\gamma Z}g_{5,L}^{H,\gamma Z}$$
$$+ (g_V^{e\,2} + g_A^{e\,2} \pm 2\lambda g_V^e g_A^e)\eta_Z g_{5,L}^{H,Z}. \quad (10)$$

In the quark-parton model, at leading-order, contributions to the SIDIS structure functions F_i and g_i can be expressed in terms of the quark (p)PDFs and the hadron FFs. In the NC

case, these functions are

$$[F_1^{H,\gamma}, F_1^{H,\gamma Z}, F_1^{H,Z}] = \frac{1}{2}\sum_q[e_q^2, 2e_q g_V^q, g_V^{q\,2} + g_A^{q\,2}]$$
$$\times (q D_q^H + \bar{q}D_{\bar{q}}^H),$$
$$[F_3^{H,\gamma}, F_3^{H,\gamma Z}, F_3^{H,Z}] = \sum_q[0, 2e_q g_A^q, 2g_V^q g_A^q]$$
$$\times (q D_q^H - \bar{q}D_{\bar{q}}^H),$$
$$[g_1^{H,\gamma}, g_1^{H,\gamma Z}, g_1^{H,Z}] = \frac{1}{2}\sum_q[e_q^2, 2e_q g_V^q, g_V^{q\,2} + g_A^{q\,2}]$$
$$\times (\Delta q D_q^H + \Delta\bar{q}D_{\bar{q}}^H),$$
$$[g_5^{H,\gamma}, g_5^{H,\gamma Z}, g_5^{H,Z}] = \sum_q[0, e_q g_A^q, g_V^q g_A^q]$$
$$\times (\Delta\bar{q}D_{\bar{q}}^H - \Delta q D_q^H),$$

$$(11)$$

where e_q is the fractional electric charge of the quark, $g_V^q = \pm\frac{1}{2} - 2e_q\sin^2\theta_W$, and $g_A^q = \pm\frac{1}{2}$, with the $+$ sign for up-type quarks and the $-$ sign for down-type quarks. In the CC case, since the W boson interacts only with certain flavours, we have (assuming four active flavours):

$$F_1^{H,W^-} = u D_d^H + \bar{d}D_{\bar{u}}^H + \bar{s}D_{\bar{c}}^H + c D_s^H,$$
$$F_3^{H,W^-} = 2(u D_d^H - \bar{d}D_{\bar{u}}^H - \bar{s}D_{\bar{c}}^H + c D_s^H),$$
$$g_1^{H,W^-} = \Delta u D_d^H + \Delta\bar{d}D_{\bar{u}}^H + \Delta\bar{s}D_{\bar{c}}^H + \Delta c D_s^H,$$
$$g_5^{H,W^-} = -\Delta u D_d^H + \Delta\bar{d}D_{\bar{u}}^H + \Delta\bar{s}D_{\bar{c}}^H - \Delta c D_s^H.$$

$$(12)$$

For W^+ exchange, one should replace $u \leftrightarrow d$ and $s \leftrightarrow c$.

3 Next-to-leading order

Assuming factorization, the polarized SIDIS structure functions $g_{1,5,L}^{H,V}$ [2] at a factorization scale μ_F can be expressed as convolutions of non-perturbative pPDFs $\Delta f_k(x, \mu_F^2)$ and FFs $D_j^H(z, \mu_F^2)$ with short-distance coefficients $\Delta C_{1,5,L}^{jk,V}(x, z, \mu_F^2)$, which can be evaluated in perturbation theory. At next-to-leading-order (NLO) in the strong coupling constant α_s these read

$$g_i^{H,V}(x, z, Q^2)$$
$$= \frac{1}{2}\sum_{q_a,q_b}\Delta\xi_i^{q_a}\Big\{\Delta C_{o_i}^V D_{q_b}^H(z, Q^2)\Delta q_a(x, Q^2)$$

---

[2] V standing for γ, Z, γZ or $W^\pm$.

$$+ \frac{\alpha_s(Q^2)}{2\pi} \big[D_{q_b}^H \otimes \Delta C_i^{qq,V} \otimes \Delta q_a$$

$$+ D_g^H \otimes \Delta C_i^{gq,V} \otimes \Delta q_a$$

$$+ D_{q_b}^H \otimes \Delta C_i^{qg,V} \otimes \Delta g \big] (x, z, Q^2) \Big\}, \tag{13}$$

where we fix all scales equal to Q. The sum runs over all contributing partonic channels. That means, for $V = \gamma, \gamma Z, Z$,

$$q_a = q_b = u, d, s, c, \bar{u}, \bar{d}, \bar{s}, \bar{c} \tag{14}$$

if we consider four active flavours, while for $V = W^-$ only

$$q_a(q_b) = u(d), \bar{d}(\bar{u}), \bar{s}(\bar{c}), c(s) \tag{15}$$

are considered. For $V = W^+$, one should replace $u \leftrightarrow d$ and $s \leftrightarrow c$. The factor $\Delta \xi_i^{q_a}$ takes the value $\Delta \xi_1^{q_a} = 1$ for every q_a, while it reads $\Delta \xi_5^{q_a} = \Delta \xi_L^{q_a} = 1$ if q_a refers to a quark and $\Delta \xi_5^{q_a} = \Delta \xi_L^{q_a} = -1$ for q_a representing an anti-quark. In Eq. (13) $\otimes$ denotes the usual convolution:

$$(D \otimes C \otimes f)(x, z, Q^2)$$

$$= \int_x^1 \frac{dy}{y} \int_z^1 \frac{d\omega}{\omega} D(\omega) C\left(\frac{x}{y}, \frac{z}{\omega}, Q^2\right)$$

$$\times f(y). \tag{16}$$

According to Eqs. (11) and (12), which represent the leading-order term of Eq. (13), the coefficients $\Delta C_{o_i}^V$ can be written as

$$\Delta C_{o_1}^V = \lambda_V^V; \qquad \Delta C_{o_5}^V = \lambda_A^V; \qquad \Delta C_{o_L}^V = 0, \tag{17}$$

with

$$\lambda_V^\gamma = e_q^2, \qquad \lambda_A^\gamma = 0, \qquad \lambda_V^{\gamma Z} = 2e_q g_V^q,$$

$$\lambda_A^{\gamma Z} = -2e_q g_A^q, \qquad \lambda_V^Z = g_V^{q\,2} + g_A^{q\,2}, \tag{18}$$

$$\lambda_A^Z = -2g_V^q g_A^q, \qquad \lambda_V^W = -\lambda_A^W = 2.$$

In order to calculate the NLO coefficients $\Delta C_i^{jk,V}$, we must take into account the one-loop corrections to the partonic process $V + q_a \to q_b$, the real emission $V + q_a \to q_b + g$ and the box contribution $V + g \to q_b + \bar{q}_b$. The first two channels contribute to the case with $jk = qq$, and the last one to $jk = qg$. The coefficient ΔC_i^{gq} is obtained from the real emission, considering that the gluon is the hadronizing parton. At the intermediate stages of the computation divergences appear. In order to regularize them we use dimensional regularization [17, 18], i.e., we work in a d-dimensional space, with $d = 4 - 2\epsilon$. All quarks are considered massless.

Once the matrix element of each channel jk has been computed, one must obtain the spin dependent amplitude

$$\Delta |M^{jk}|_{\mu\nu}^2 = \frac{1}{2} \big[|M_+^{jk}|_{\mu\nu}^2 - |M_-^{jk}|_{\mu\nu}^2 \big], \tag{19}$$

defined in terms of the amplitudes for partons whose polarization is parallel $(+)$ or anti-parallel $(-)$ to that of the target. The calculation of each term in Eq. (19) requires projection onto definite helicity states of the incoming particles. It is then necessary to make use of the relations

$$u(p, \lambda)\bar{u}(p, \lambda) = \frac{1 + \lambda \gamma_5}{2} \not{p} \tag{20}$$

for incoming quarks with helicity λ (a similar expression is obtained for anti-quarks) and

$$\varepsilon_\alpha(p, \lambda_g)\varepsilon_\beta^*(p, \lambda_g) = \frac{1}{2(1-\epsilon)} \left[-g_{\alpha\beta} + \frac{p_\alpha \eta_\beta + p_\beta \eta_\alpha}{p.\eta} \right]$$

$$+ \frac{1}{2} i \lambda_g \epsilon_{\alpha\beta\rho\sigma} \frac{p^\rho \eta^\sigma}{p.\eta} \tag{21}$$

for incoming gluons with helicity λ_g, where η is an arbitrary light-like momentum, provided that $p.\eta \neq 0$. The terms independent of λ and λ_g in Eqs. (20) and (21) respectively contribute only to the unpolarized amplitude (since they cancel out when subtracting the two terms in Eq. (19)). In the last case, the averaging of gluon spins in d dimensions should be performed by dividing by the $d - 2 = 2(1 - \epsilon)$ possible spin orientations, as has been made explicit in Eq. (21).

Once the NLO $\Delta |M^{jk}|_{\mu\nu}^2$ has been computed, we can obtain each one of the coefficients $\Delta C_i^{jk,V}$ as the finite part of the *partonic structure function*, defined by

$$g_i^{jk} = \frac{1}{4\pi} \int d\Gamma \tilde{P}_i^{\mu\nu} \Delta |M^{jk}|_{\mu\nu}^2, \tag{22}$$

where $d\Gamma$ is the d-dimensional phase-space and the projectors $\tilde{P}_i^{\mu\nu}$ are

$$\tilde{P}_1^{\mu\nu} = -i\epsilon^{\mu\nu\rho\sigma} \frac{q_\rho p_\sigma}{2p \cdot q}, \qquad \tilde{P}_L^{\mu\nu} = \frac{4x^2}{Q^2} p^\mu p^\nu,$$

$$\tilde{P}_5^{\mu\nu} = \frac{1}{2(1-\epsilon)} \big[-g^{\mu\nu} + \tilde{P}_L^{\mu\nu} \big]. \tag{23}$$

The functions g_i^{jk} contain collinear divergences, which appear as poles in ϵ (at NLO, simple poles in ϵ). We factorize these divergences using the $\overline{MS}$ scheme, i.e., removing the

quantities

$$\tilde{g}_i^{qq}(x,z) = \Delta C_{o_i} \left[-\frac{1}{\epsilon} + \gamma_E - \log(4\pi) \right]$$
$$\times \left[\Delta f_{qq}(x)\delta(1-z) + P_{qq}(z)\delta(1-x) \right],$$

$$\tilde{g}_i^{qg}(x,z) = \Delta C_{o_i} \left[-\frac{1}{\epsilon} + \gamma_E - \log(4\pi) \right] \Delta P_{qg}(x)\delta(1-z),$$

$$\tilde{g}_i^{gq}(x,z) = \Delta C_{o_i} \left[-\frac{1}{\epsilon} + \gamma_E - \log(4\pi) \right] P_{gq}(z)\delta(1-x),$$

(24)

where P_{jk} and ΔP_{jk} are the unpolarized and polarized LO Altarelli–Parisi splitting functions [19] and $\gamma_E = 0,5772\ldots$ is the Euler constant. The quantity Δf_{qq} is defined below in Eq. (31). The finite functions obtained after factorization are the coefficients ΔC_i^{jk}.

The main feature of the calculation described above is the correct use of γ_5 and the Levi-Civita tensor appearing in Eqs. (20) and (21), which is not straightforward in $d \neq 4$ dimensions. For our calculations we use the original prescription of 't Hooft and Veltman [18], afterwards systematized by Breitenlohner and Maison [20] (HVBM scheme), which is the most reliable and consistent scheme [20, 21].

In the HVBM scheme explicit definitions for γ_5 and $\epsilon_{\mu\nu\rho\sigma}$ are given. In particular,

$$\gamma_5 = \frac{i}{4!} \epsilon^{\mu\nu\rho\sigma} \gamma_\mu \gamma_\nu \gamma_\rho \gamma_\sigma,$$

(25)

and the ϵ-tensor is regarded as a genuinely four-dimensional object with its components vanishing in all unphysical dimensions. The d-dimensional Minkowski space is then explicitly divided into two subspaces, a four-dimensional one and a $(d-4)$-dimensional one, each of them equipped with its metric tensor, $\tilde{g}$ and $\hat{g}$ respectively. The Dirac matrices are also split into a four-dimensional and a $(d-4)$-dimensional part:

$$\gamma_\mu = \tilde{\gamma}_\mu + \hat{\gamma}_\mu.$$

(26)

Each part satisfies the usual anticommutation relation.

As defined above, γ_5 anticommutes with $\tilde{\gamma}_\mu$ but commutes with $\hat{\gamma}_\mu$. As a result, besides the usual scalar products $p' \cdot p'$ (p' being the moment of the outgoing parton), products $\hat{p}' \cdot \hat{p}'$ show up in calculations, with $\hat{p}'$ the $(d-4)$-dimensional component of the momentum p'. Every time this type of products appear, the two-particle phase space in Eq. (22) must be used in the less integrated form [22]

$$d\Gamma = \frac{1}{8\pi}(4\pi)^\epsilon \frac{-\epsilon}{\Gamma(1-\epsilon)} \int_0^{sz(1-z)} d(\hat{p}'^2)(\hat{p}'^2)^{-(1+\epsilon)}.$$

(27)

For those terms which are independent of $\hat{p}'^2$ the integration is trivial and one recovers the result of [9].

When computing the amplitudes, γ_5 matrices are present not only due to the helicity projectors, but also because of the weak interaction vertex. With the definition of γ_5 given in the HVBM scheme, it is important to consistently define the couplings with the chiral fields. It is shown in Ref. [23] that the correct W^- vertex is obtained through the symmetrization

$$\gamma^\mu(1-\gamma_5) \to \frac{1}{2}(1+\gamma_5)\gamma^\mu(1-\gamma_5) = \tilde{\gamma}^\mu(1-\gamma_5). \quad (28)$$

Analogously, the Z vertex is obtained by

$$\gamma^\mu(g_V^q - g_A^q\gamma_5) = \gamma^\mu(g_V^q - g_A^q) + g_A^q\gamma^\mu(1-\gamma_5)$$
$$\to \gamma^\mu(g_V^q - g_A^q) + g_A^q\tilde{\gamma}^\mu(1-\gamma_5). \quad (29)$$

Finally, an important property of the HVBM prescription for γ_5 is that it leads to helicity non-conservation at the qqg vertex in d dimensions, expressed by a non-vanishing difference of unpolarized and polarized d-dimensional LO quark-to-quark splitting functions,

$$\Delta P_{qq}^{d=4-2\epsilon}(x) - P_{qq}^{d=4-2\epsilon}(x) = 4C_F\epsilon(1-x). \quad (30)$$

As is discussed in [24–26], this result entails some disagreeable consequences, such as non-conservation of the flavour non-singlet axial current and an incorrect result for the $\mathcal{O}(\alpha_s)$ correction to the Bjørken sum rule. It is then customary to slightly modify the definition of the $\overline{\text{MS}}$ scheme in the polarized case and define the quantity

$$\Delta f_{qq}(x) = \Delta P_{qq}(x) + 4C_F\epsilon(1-x) \quad (31)$$

to be removed in Eq. (24).

We present now the NLO coefficients ΔC_i^{jk}. All the traces have been computed with the program TRACER [27], which masters most of the intricacies of HVBM scheme. All results are given in the $\overline{\text{MS}}$ scheme, as defined above. Here, $\mu_F^{IS} = \mu_F^{FS} = \mu_F$ is made, with μ_F^{IS} and μ_F^{FS} the initial state and final state factorization scales respectively. For the sake of brevity we suppress in the following results the argument (x, z) of the coefficient functions. For $i = 1$,

$$\Delta C_1^{qq,V} = C_1^{qq,V} - \lambda_V^V C_F 2(1-x)(1-z), \quad (32)$$

$$\Delta C_1^{qg,V} = \lambda_V^V \frac{1}{2} \left\{ \delta(1-z) \left[\Delta\tilde{P}_{qg}(x) \log\left(\frac{Q^2}{\mu_F^2}\frac{1-x}{x}\right) \right. \right.$$
$$\left. + 2(1-x) \right] + \Delta\tilde{P}_{qg}(x) \left[\frac{1}{(1-z)_+} + \frac{1}{z} - 2 \right] \right\},$$

(33)

$$\Delta C_1^{gq,V} = C_1^{gq,V} - \lambda_V^V C_F 2(1-x)z; \quad (34)$$

for $i = 5$

$$\Delta C_5^{qq,V} = \frac{\lambda_A^V}{\lambda_V^V} C_1^{qq,V},$$

$$\Delta C_5^{qg,V} = \lambda_A^V \left[\frac{\Delta C_1^{qg,V}}{\lambda_V^V} - \Delta P_{qg}(x) 2 \frac{1-z}{z} \right], \quad (35)$$

$$\Delta C_5^{gq,V} = \frac{\lambda_A^V}{\lambda_V^V} C_1^{gq,V};$$

and finally, the longitudinal coefficients are

$$\Delta C_L^{qq,V} = \frac{\lambda_A^V}{\lambda_V^V} C_L^{qq,V}, \qquad \Delta C_L^{qg,V} = 0,$$

$$\Delta C_L^{gq,V} = \frac{\lambda_A^V}{\lambda_V^V} C_L^{gq,V}. \qquad (36)$$

The functions C_i^{jk} are the unpolarized coefficients and are shown in Appendix A. The factors λ_A^V and λ_V^V are given in Eq. (18). The quantity $\Delta \tilde{P}_{qg}$ is defined for simplicity as

$$\Delta \tilde{P}_{qg}(x) = 2\Delta P_{qg}(x) = 2x - 1. \qquad (37)$$

Finally, the coefficients ΔC_4^{jk} can be obtained as

$$\Delta C_4^{jk,V} = \Delta C_L^{jk,V} + 2x \Delta C_5^{jk,V}. \qquad (38)$$

We note that the results for the electromagnetic case ($\Delta C_i^{jk,\gamma}$) are in agreement with those of Ref. [10].

Finally, we make some comments on the unpolarized case. It is convenient to define

$$(\mathcal{F}_1, \mathcal{F}_2, \mathcal{F}_3) = (2F_1, F_2/x, F_3) \qquad (39)$$

and

$$\mathcal{F}_L = \mathcal{F}_2 - \mathcal{F}_1 = F_L/x, \qquad (40)$$

and thus, the structure functions can be written at NLO as

$$\mathcal{F}_i^{H,V}(x, z, Q^2) = \sum_{q_a, q_b} \xi_i^{q_a} \Big\{ C_{o_i}^V D_{q_b}^H(z, Q^2) q_a(x, Q^2)$$

$$+ \frac{\alpha_s(Q^2)}{2\pi} \big[D_{q_b}^H \otimes C_i^{qq,V} \otimes q_a$$

$$+ D_g^H \otimes C_i^{gq,V} \otimes q_a$$

$$+ D_{q_b}^H \otimes C_i^{qg,V} \otimes g \big](x, z, Q^2) \Big\}, \qquad (41)$$

with

$$C_{o_1}^V = \lambda_V^V; \qquad C_{o_3}^V = -\lambda_A^V; \qquad C_{o_L}^V = 0. \qquad (42)$$

The factor $\xi_i^{q_a}$ takes the value $\xi_1^{q_a} = 1$ for every q_a, while it is $\xi_3^{q_a} = \xi_L^{q_a} = 1$ if q_a refers to a quark and $\xi_3^{q_a} = \xi_L^{q_a} = -1$ for q_a representing an anti-quark.

The computation of these coefficients is similar to the polarized ones. In this case, the spin-averaged amplitude must be used, and the projectors are

$$P_L^{\mu\nu} = \frac{8x^2}{Q^2} p^\mu p^\nu, \qquad P_1^{\mu\nu} = \frac{1}{1-\epsilon} \left(-g^{\mu\nu} + \frac{1}{2} P_L^{\mu\nu} \right),$$

$$P_3^{\mu\nu} = i\epsilon^{\mu\nu\rho\sigma} \frac{q_\rho p_\sigma}{p \cdot q}. \qquad (43)$$

The same care as in the polarized case must be taken when dealing with the γ_5 matrices present in the weak vertices. All NLO $\overline{MS}$ coefficient functions $C_i^{jk,V}$ are collected in Appendix A.

4 Structure functions at an EIC

In this section we analyze the relevance of the NLO corrections to the SIDIS structure functions we have computed. We focus on the CC case, i.e. the interaction via a W^- boson, since it allow us to achieve a full flavour separation.

According to Chap. 1.12 of [5], which we follow closely, precise measurements of polarized CC structure functions are feasible at an EIC with a relatively modest integrated luminosity. The γZ structure functions become also accessible at the highest luminosities and center of mass energies. Neither of them have ever been measured. Proposed EIC parameters allow for electron energies between 5 and 30 GeV and ion energies of 50 to 325 GeV. In particular, configurations of E_e [GeV] $\times E_{ion}$ [GeV] with 20×325 and 20×250 are considered in Sect. 1.12 of [5]. The values of x and Q^2 that we use for the phenomenological analysis are compatible with either of those configurations. Based on an expected five year run time, we can consider an effective integrated luminosity of 100 fb^{-1} for NC processes and 10 fb^{-1} for CC.

We focus now on the NLO corrections to the SIDIS structure functions. We will study their behaviour for an energy scale of $Q^2 = 100$ GeV^2, for which the x-range foreseen is approximately $4.10^{-3} < x < 1$ (see Fig. 7.16 of Ref. [5]). We will consider four bins in the hadronic variable z, with $0.1 < z < 0.8$ and rely on the DSS fragmentation functions set of [28].

In Fig. 1 we show the spin dependent structure functions $g_1^{\pi^-, W^-}$, $g_5^{\pi^-, W^-}$, and $g_4^{\pi^-, W^-}/(2x)$, at $Q^2 = 100$ GeV^2 for the bin $z = 0.2$–0.4, using the DSSV set of pPDFs [4]. Results are shown both at LO (dashed) and NLO (solid). It is important to mention that NLO pPDFs are used also at LO, in order to pick up only the effect of the corrections introduced by the NLO coefficients. One observes that the
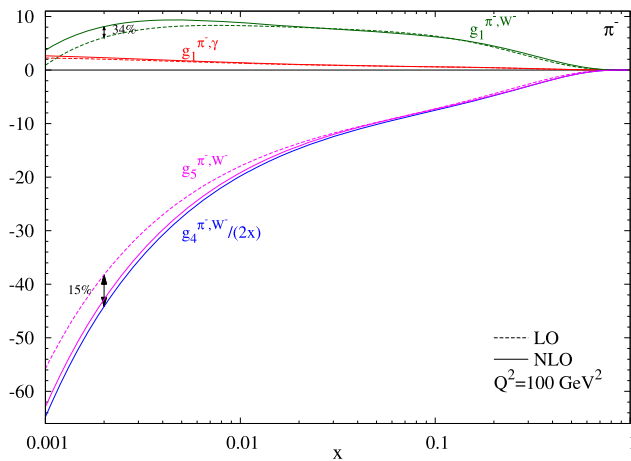
Fig. 1 CC spin dependent SIDIS structure functions $g_1^{\pi^-,W^-}$, $g_5^{\pi^-,W^-}$, and $g_4^{\pi^-,W^-}/(2x)$, at $Q^2 = 100$ GeV^2 for the z-bin $z = 0.2$–0.4. The *dashed lines* show the LO results (the one for $g_4^{\pi^-,W^-}/(2x)$ coincides with that for $g_5^{\pi^-,W^-}$), while the *solid curves* are NLO. For comparison, we also show the electromagnetic $g_1^{\pi^-,\gamma}$

NLO results differ from the LO description, particularly in the small-x range. At $x = 0.002$, for instance, the discrepancies are of about 34 % for g_1 and 15 % for $g_4/(2x)$ (these being larger than those for g_5 for all x). Thus, the NLO description is crucial for a precise extraction of the pPDFs in the small-x region, which is particularly interesting since it could be measured at the EIC with unprecedented precision. For comparison, we also show the electromagnetic $g_1^{\pi^-,\gamma}$, for which the NLO corrections are more moderate (below 15 % in the mentioned x value).

In Fig. 2 we present the prediction for the NLO SIDIS structure functions g_1^{H,W^-} with $H = \pi^\pm, K^\pm$ for the four z-bins considered. In all cases, the DSSV set of pPDFs where used. We can understand the behaviour of these structure functions, at least qualitatively, by considering the behaviour of pPDFs and FFs, taking into account that only the four channels of Eq. (15) must be considered, as is discussed next.

We focus now on the π^- case. The production of this hadron in the final state is mostly due to the hadronization of a quark d (between 30 % and 46 %) or a quark $\bar{u}$ (between 28 % and 41 %). This means that the quark present in the initial state must be a quark u or $\bar{d}$ respectively. Thus, the behaviour of the structure function is dominated by that of the Δu and $\Delta \bar{d}$ pPDFs, the first of them being positive for all x-range, and the last one negative. Given that the larger contribution is that of the u channel, the π^- structure function $g_1^{\pi^-,W^-}$ is always positive. For π^+, however, at low x contributions from $\Delta \bar{d}$ and $\Delta \bar{s}$ (negative both) are larger and so $g_1^{\pi^+,W^-}$ becomes negative.

On the other hand, given the magnitude of the fragmentation functions in DSS set,[3] the K^- production for low z is dominated by the hadronization of a quark $\bar{c}$ (around 60 %), meaning that the process is initiated by an $\bar{s}$ quark. Thus, the shape of $g_1^{K^-,W^-}$ is practically that of the $\Delta \bar{s}$ distribution, with a sign change in the DSSV set around $x \sim 0.02$. For $0.4 < z < 0.6$ the $\bar{c}$ and $\bar{u}$ hadronization probabilities are comparable, and for $0.6 < z < 0.8$ the last one is even larger, but cancellations between Δu and $\Delta \bar{d}$ occur such that the behaviour of $g_1^{K^-,W^-}$ remains very similar to that just described.

In Fig. 3 we show the prediction for the SIDIS structure functions g_5^{H,W^-} at NLO. By looking at Eq. (12) we can note that the main difference for these structure functions with respect to the previous discussion relies in the fact that these ones depend on $(-\Delta u)$, $\Delta \bar{d}$ and $\Delta \bar{s}$, all of them basically negative for the whole x-range (except for $\Delta \bar{s}$, which is positive for large x, but that effect is not noticeable). That explains why g_5^{H,W^-} is negative for all hadrons considered ($H = \pi^\pm, K^\pm$) and for all x values.

As was explained above, the $g_1^{K^-,W^-}$ structure function behaviour is closely related to the $\Delta \bar{s}$ distribution. Thus, one can expect it to be sensitive to a small change in that pPDF. We show in the left hand side of Fig. 4 the CC and electromagnetic structure functions $g_1^{K^-,W^-}$ (green) and $g_1^{K^-,\gamma}$ (red) calculated with the DSSV set of pPDFs (solid) and the same result after modifying *only* the $\Delta \bar{s}$ distribution according to the one in the DNS set [30] (dashed), as a way to emphasize the sensitivity of the observable on that flavour. We note large discrepancies between both sets of pPDFs in the CC case, and even observe a region in which they have opposite signs, unlike the electromagnetic case, for which the difference between both sets is much smaller. In the last case, the presence of an $\bar{s}$ quark in the initial state implies (at LO) the hadronization of an $\bar{s}$ quark, but its FF into a K^- hadron is almost negligible. The sensitivity of $g_1^{K^-,W^-}$ is also stronger than that of the DIS structure function $g_1^{W^-}$ for some x-ranges as can be observed in the right hand side of Fig. 4.

Similarly, one can expect the $g_1^{\pi^-,W^-}$ structure function to be particularly sensitive to a variation of Δu. We show in the left hand side of Fig. 5 the CC and electromagnetic spin dependent structure functions $g_1^{\pi^-,W^-}$ (green) and $g_1^{\pi^-,\gamma}$ (red) respectively, calculated using DSSV pPDFs set (solid) and DSSV set with the exception of Δu, taken from DNS set (dashed). By comparing these two plots, we can note that in fact the CC SIDIS structure function is much more sensitive to Δu than the electromagnetic one, and thus better flavour separation can be achieved from such measurement.

---

[3]The same being valid for other sets of FFs [29].

Fig. 2 CC spin dependent structure function g_1^{H,W^-} for $H = \pi^\pm, K^\pm$ at $Q^2 = 100$ GeV^2 for four different z-bins
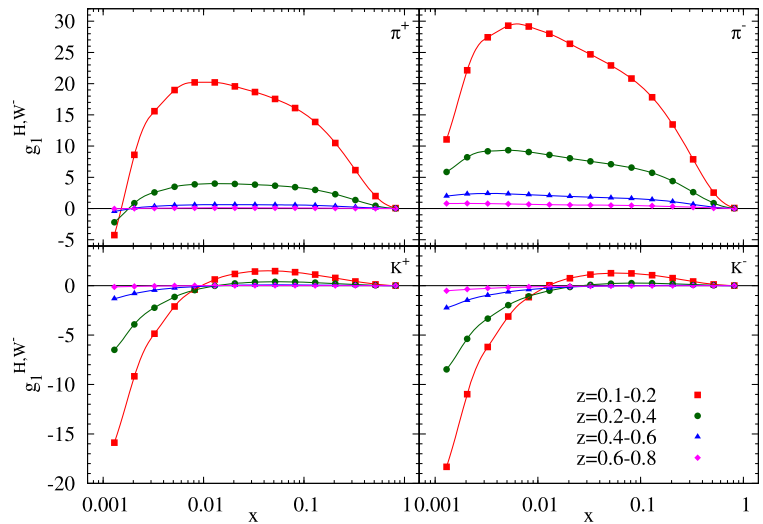
Fig. 3 CC spin dependent structure function g_5^{H,W^-} for $H = \pi^\pm, K^\pm$ at $Q^2 = 100$ GeV^2 for four different z-bins
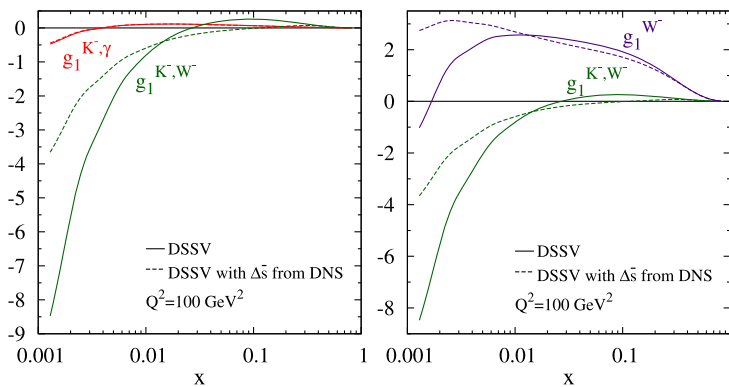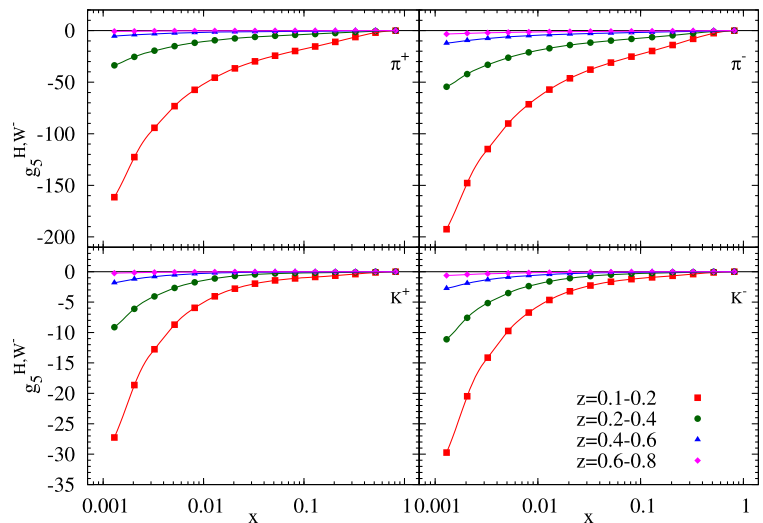
Fig. 4 *Left*: CC and electromagnetic spin dependent SIDIS structure functions $g_1^{K^-,W^-}$ (*green*) and $g_1^{K^-,\gamma}$ (*red*) for $z = 0.2$–0.4. We present the results obtained using DSSV pPDFs set (*solid*) and all pPDFs of DSSV set except for $\Delta\bar{s}$, taken from DNS set (*dashed*). *Right*: The same, for CC spin dependent SIDIS structure functions $g_1^{K^-,W^-}$ for $z = 0.2$–0.4 (*green*) and DIS structure function $g_1^{W^-}$ (*violet*) (Color figure online)
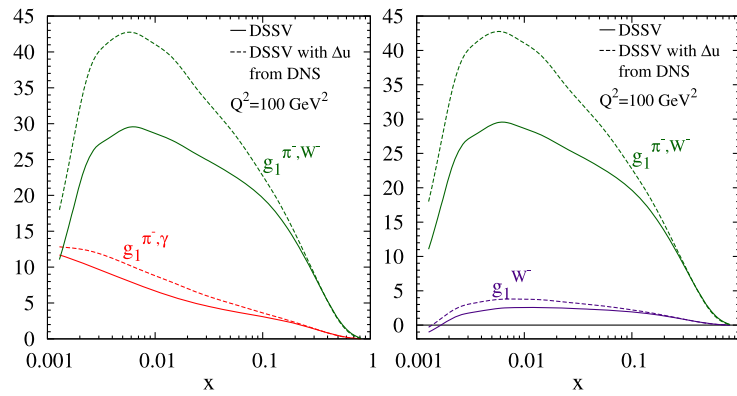
Fig. 5 *Left*: CC and electromagnetic spin dependent structure functions $g_1^{\pi^-,W^-}$ (*green*) and $g_1^{\pi^-,\gamma}$ (*red*) respectively, calculated using DSSV pPDFs set (*solid*) and DSSV set except for Δu, which is taken from DNS set (*dashed*). In both cases, we use $z = 0.1$–0.2. *Right*: The same for CC spin dependent SIDIS structure functions $g_1^{\pi^-,W^-}$ for $z = 0.1$–0.2 (*red*) and DIS structure function $g_1^{W^-}$ (*violet*) (Color figure online)

We also compare in the right hand side of Fig. 5 the CC spin dependent SIDIS structure functions $g_1^{\pi^-,W^-}$ for $z = 0.2$–0.4 (red) and DIS structure function $g_1^{W^-}$ (violet) obtained using DSSV pPDFs set (solid) and DSSV set with the exception of Δu, taken from DNS set (dashed). The sensitivity of these functions on Δu are similar, but one can still profit from the larger structure function in the SIDIS case.

Concerning the feasibility of the extraction of the electroweak structure functions, experimentally one has access to them through the asymmetries, which depend both in polarized and unpolarized structure functions. In order to estimate the statistical uncertainties that one might expect in such measurements, we can rely on the estimation for the fully inclusive ones (δA_I) performed in [5].[4]

As a first approach to estimate the statistical uncertainties, we can make use of the simple relation $\delta A_{SI}^H \sim \dfrac{\delta A_I}{\sqrt{D_{dom}^H}}$

for each z-bin, where δA_{SI}^H is the relative uncertainty on the asymmetry for the semi-inclusive case and D_{dom}^H refers to the integral of the leading fragmentation function for the hadron H over the corresponding z-bin. For CC processes, the semi-inclusive uncertainties (for $\pi^\pm$ and $K^\pm$) turn out to be smaller than 15 % all the way down to $x \sim 10^{-2}$ for $0.1 < z < 0.2$. The uncertainties grow for larger values of z, reaching the same level of accuracy in the $0.6 < z < 0.8$ bin only at $x \sim 0.05$. Given that some of the electroweak unpolarized semi-inclusive structure functions will also be first determined at the EIC and that the beam energies of the collider have not been decided yet, we believe it is early to attempt for a precise estimation of the uncertainties that can

be achieved for all possible combinations of polarized structure functions. Nevertheless, the numbers discussed above are enough to emphasize that one might expect uncertainties of the same level or (for most of the cases) smaller than the size of the computed NLO corrections in the polarized structure functions, making crucial to carry out the analysis to the perturbative accuracy presented in this paper.

5 Conclusions

We have computed the next-to-leading order QCD corrections to the complete set of polarized semi-inclusive electroweak structure functions in a consistent scheme.

We have performed a phenomenological study of possible measurements in an EIC. The NLO corrections are found to be important in the small-x range, the kinematical region of particular interest at a high energy collider.

We analyzed the sensitivity of SIDIS CC structure functions on different pPDFs, and showed that they provide an excellent tool to disentangle the full set of flavour spin dependent distributions with an unprecedented precision by including the electroweak polarized SIDIS structure functions. In particular, we explicitly show that the structure function $g_1^{K^-,W^-}$ is sensitive to the very poorly known $\Delta\bar{s}$ distribution while the function $g_1^{\pi^-,W^-}$ is particularly sensitive to Δu.

---

[4]The asymmetries are defined in Eq. (1.14) of Sect. 1.12 in [5] and involve a combination of different polarized and unpolarized structure functions.

Appendix A: Unpolarized SIDIS coefficient functions

Here we list all unpolarized coefficients $C_i^{jk,V}$ for SIDIS as introduced in Sect. 3. To keep the expressions as short as possible we define

$$
\tilde{P}_{qq}(\xi) = \frac{1}{C_F} P_{qq}, \qquad \tilde{P}_{qg}(\xi) = 2P_{qg}(\xi),
$$

$$
\tilde{P}_{gq}(\xi) = \frac{1}{C_F} P_{gq}(\xi),
$$

$$
L_1(\xi) = \left(1+\xi^2\right)\left(\frac{\log(1-\xi)}{1-\xi}\right)_+,
$$

$$
L_2(\xi) = \frac{1+\xi^2}{1-\xi}\log\xi. \tag{A.1}
$$

In what follows, we always suppress the argument (x,z) of the coefficient functions. All results presented here are given in the $\overline{\text{MS}}$ scheme.

The unpolarized coefficients $C_i^{jk,V}$ for SIDIS are

$$
\begin{aligned}
C_1^{qq,V} = \lambda_V^V C_F \Bigg\{ &-8\delta(1-x)\delta(1-z) \\
&+ \delta(1-x)\left[\tilde{P}_{qq}(z)\log\left(\frac{Q^2}{\mu_F^2}\right) + L_1(z)\right. \\
&\left. + L_2(z) + (1-z)\right] \\
&+ \delta(1-z)\left[\tilde{P}_{qq}(x)\log\left(\frac{Q^2}{\mu_F^2}\right) + L_1(x)\right. \\
&\left. - L_2(x) + (1-x)\right] + 2\frac{1}{(1-x)_+}\frac{1}{(1-z)_+} \\
&- \frac{1+z}{(1-x)_+} - \frac{1+x}{(1-z)_+} + 2(1+xz)\Bigg\}, \tag{A.2}
\end{aligned}
$$

$$
\begin{aligned}
C_1^{qg,V} = \lambda_V^V \frac{1}{2}\Bigg\{ &\delta(1-z)\left[\tilde{P}_{qg}(x)\log\left(\frac{Q^2}{\mu_F^2}\frac{1-x}{x}\right)\right. \\
&\left. + 2x(1-x)\right] \\
&+ \tilde{P}_{qg}(x)\left[\frac{1}{(1-z)_+} + \frac{1}{z} - 2\right]\Bigg\}, \tag{A.3}
\end{aligned}
$$

$$
\begin{aligned}
C_1^{gq,V} = \lambda_V^V C_F \Bigg\{ &\tilde{P}_{gq}(z)\left[\delta(1-x)\log\left(\frac{Q^2}{\mu_F^2}z(1-z)\right)\right. \\
&\left. + \frac{1}{(1-x)_+}\right] + z\delta(1-x) + 2(1+x-xz) \\
&- \frac{1+x}{z}\Bigg\}; \tag{A.4}
\end{aligned}
$$

$$
C_L^{qq,V} = \lambda_V^V 4C_F xz, \tag{A.5}
$$

$$
C_L^{qg,V} = \lambda_V^V 4x(1-x), \tag{A.6}
$$

$$
C_L^{gq,V} = \lambda_V^V 4C_F x(1-z); \tag{A.7}
$$

$$
C_3^{qq,V} = -\lambda_A^V\left[\frac{C_1^{qq,V}}{\lambda_V^V} - C_F 2(1-x)(1-z)\right], \tag{A.8}
$$

$$
C_3^{qg,V} = -\lambda_A^V\left[\frac{C_1^{qg,V}}{\lambda_V^V} - 2P_{qg}(x)\frac{1-z}{z}\right], \tag{A.9}
$$

$$
C_3^{gq,V} = -\lambda_A^V\left[\frac{C_1^{gq,V}}{\lambda_V^V} - C_F 2(1-x)z\right]. \tag{A.10}
$$

We note that all our results in Eqs. (A.2)–(A.10) are in agreement with Refs. [9, 10].

Appendix B: Unpolarized and polarized DIS coefficient functions

For the sake of completeness, we present the NLO unpolarized and polarized DIS structure functions, F_i^V and g_i^V respectively. These, can be expressed as convolutions of non-perturbative (p)PDFs with short-distance coefficients ($C_{1,3,L}^{j,V}(x,Q^2)$ in the unpolarized case and $\Delta C_{1,5,L}^{j,V}(x,Q^2)$ in the polarized one). At NLO, these read

$$
\begin{aligned}
\mathcal{F}_i^V(x,Q^2) = \frac{1}{2}\sum_{q_a}\xi_i^{q_a}\Bigg\{ &C_{o_i}^V q_a(x,Q^2) + \frac{\alpha_s(Q^2)}{2\pi} \\
&\times\left[C_i^{q,V}\otimes q_a + C_i^{g,V}\otimes g\right](x,Q^2)\Bigg\}, \tag{B.1}
\end{aligned}
$$

$$
\begin{aligned}
g_i^V(x,Q^2) = \frac{1}{2}\sum_{q_a}\Delta\xi_i^{q_a}\Bigg\{ &\Delta C_{o_i}^V\Delta q_a(x,Q^2) + \frac{\alpha_s(Q^2)}{2\pi} \\
&\times\left[\Delta C_i^{q,V}\otimes\Delta q_a + \Delta C_i^{g,V}\otimes\Delta g\right](x,Q^2)\Bigg\}. \tag{B.2}
\end{aligned}
$$

All the relevant factors have been introduced in Sect. 3.

The unpolarized coefficients are

$$
C_L^{q,V} = \lambda_V^V C_F 2x,
$$

$$
\begin{aligned}
C_1^{q,V} = \lambda_V^V C_F\Bigg\{ &\log\left(\frac{Q^2}{\mu_F^2}\right)\tilde{P}_{qq}(x) + \delta(1-x)\left(-\frac{9}{2} - \frac{\pi^2}{3}\right) \\
&+ L_1(x) - L_2(x) - \frac{3}{2}\frac{1}{(1-x)_+} + 3\Bigg\},
\end{aligned}
$$

$$
C_3^{q,V} = -\lambda_A^V\left[\frac{C_1^{q,V}}{\lambda_V^V} - C_F(1-x)\right], \tag{B.3}
$$

$$
C_L^{g,V} = \lambda_V^V 2x(1-x),
$$

$$
C_1^{g,V} = \lambda_V^V\frac{1}{2}\Bigg\{\tilde{P}_{qg}(x)\left[\log\left(\frac{Q^2}{\mu_F^2}\frac{1-x}{x}\right) - 1\right] + 2x(1-x)\Bigg\},
$$

$$
C_3^{g,V} = 0;
$$

and the polarized ones,

$$\Delta C_L^{q,V} = \frac{\lambda_A^V}{\lambda_V^V} C_L^{q,V}$$

$$\Delta C_1^{q,V} = C_1^{q,V} - \lambda_V^V C_F (1-x),$$

$$\Delta C_5^{q,V} = \frac{\lambda_A^V}{\lambda_V^V} C_1^{q,V},$$

$$\Delta C_L^{g,V} = 0,$$
$(B.4)$

$$\Delta C_1^{g,V} = \lambda_V^V \frac{1}{2} \left\{ \Delta \tilde{P}_{qg} \left[\log\left(\frac{Q^2}{\mu_F^2} \frac{1-x}{x} \right) - 1 \right] + 2(1-x) \right\},$$

$$\Delta C_3^{g,V} = 0,$$

with $L_1(x)$, $L_2(x)$ and $\tilde{P}_{jk}$ defined in Eq. (A.1) and $\Delta \tilde{P}_{jk}$ defined in Eq. (37).

All our results are in agreement with Refs. [9, 22, 31, 32].

References

1. M. Burkardt, C.A. Miller, W.D. Nowak, Rep. Prog. Phys. **73**, 016201 (2010)
2. D. de Florian, R. Sassot, M. Stratmann, W. Vogelsang, Prog. Part. Nucl. Phys. **67**, 251 (2012)
3. D. de Florian, R. Sassot, M. Stratmann, W. Vogelsang, Phys. Rev. D **80**, 034030 (2009)
4. D. de Florian, R. Sassot, M. Stratmann, W. Vogelsang, Phys. Rev. Lett. **101**, 072001 (2008)
5. D. Boer, M. Diehl, R. Milner, R. Venugopalan, W. Vogelsang, D. Kaplan, H. Montgomery, S. Vigdor et al., arXiv:1108.1713 [nucl-th]
6. B. Lampe, Phys. Lett. B **227**, 469 (1989)
7. W. Vogelsang, A. Weber, Nucl. Phys. B **362**, 3 (1991)
8. P. Mathews, V. Ravindran, Phys. Lett. B **278**, 175 (1992)
9. G. Altarelli, R.K. Ellis, G. Martinelli, S.-Y. Pi, Nucl. Phys. B **160**, 301 (1979)
10. D. de Florian, M. Stratmann, W. Vogelsang, Phys. Rev. D **57**, 5811 (1998)
11. M. Anselmino, P. Gambino, J. Kalinowski, Z. Phys. C **64**, 267 (1994)
12. J. Beringer et al. (Particle Data Group Collaboration), Phys. Rev. D **86**, 010001 (2012)
13. L. Trentadue, G. Veneziano, Phys. Lett. B **323**, 201 (1994)
14. D. Graudenz, Nucl. Phys. B **432**, 351 (1994)
15. D. de Florian, C.A. Garcia Canal, R. Sassot, Nucl. Phys. B **470**, 195 (1996)
16. C.G. Callan Jr., D.J. Gross, Phys. Rev. Lett. **22**, 156 (1969)
17. C.G. Bollini, J.J. Giambiagi, Nuovo Cimento B **12**, 20 (1972)
18. G. 't Hooft, M.J.G. Veltman, Nucl. Phys. B **44**, 189 (1972)
19. G. Altarelli, G. Parisi, Nucl. Phys. B **126**, 298 (1977)
20. P. Breitenlohner, D. Maison, Commun. Math. Phys. **52**, 11 (1977)
21. G. Bonneau, Phys. Lett. B **96**, 147 (1980)
22. W. Vogelsang, Z. Phys. C **50**, 275 (1991)
23. J.G. Korner, N. Nasrallah, K. Schilcher, Phys. Rev. D **41**, 888 (1990)
24. R. Mertig, W.L. van Neerven, Z. Phys. C **70**, 637 (1996)
25. W. Vogelsang, Phys. Rev. D **54**, 2023 (1996)
26. W. Vogelsang, Nucl. Phys. B **475**, 47 (1996)
27. M. Jamin, M.E. Lautenbacher, Comput. Phys. Commun. **74**, 265 (1993)
28. D. de Florian, R. Sassot, M. Stratmann, Phys. Rev. D **75**, 114010 (2007)
29. S. Albino, B.A. Kniehl, G. Kramer, Nucl. Phys. B **725**, 181 (2005)
30. D. de Florian, G.A. Navarro, R. Sassot, Phys. Rev. D **71**, 094018 (2005)
31. G. Altarelli, R.K. Ellis, G. Martinelli, Nucl. Phys. B **157**, 461 (1979)
32. D. de Florian, R. Sassot, Phys. Rev. D **51**, 6052 (1995)